

DESIGN AND IMPLEMENTATION OF NON-INVASIVE PROFILE MONITORS FOR THE ESS LEBT

C.A. Thomas*, T. Gahl, T. Grandsaert, H. Kocevar,
H. Lee, A. Serrano, T. Shea, European Spallation Source ERIC, Lund, Sweden

Abstract

We present in this paper the design and implementation of the Non-invasive Profile Monitors for the ESS LEBT. Non-invasive Profile Monitors at ESS measure the transverse profile of the high power proton beam. As such the NPM for the LEBT is not different from NPM designed for other sections of the ESS linac, however, it received the requirement to measure the position of the beam accurately with respect to the centre of the vacuum chamber, representing the reference orbit. This particular requirement led to implement a specific design to provide absolute position measurement to the system. In the following we will first describe the design and the associated functionalities, and then we will present the performance measurements of this built system, fully integrated into the control system. Finally we will discuss the performance in comparison to the initial requirements.

INTRODUCTION

For the commissioning and operation of the ESS source and LEBT, beam transverse profile and r.m.s size are required for the characterisation of the beam lattice along the LEBT and at the entrance of the RFQ. In addition beam position and angle at the entrance of the RFQ is also required. For the measurement of the beam transverse profile and size, Non-invasive Profile Monitors (NPM) have been designed. An NPM for ESS consists of two 1D profile measurements, based on the interaction's by-product of the vacuum chamber residual gas with the accelerated protons. For the LEBT NPM, the beam profile is measured by means of two imaging systems, using the induced gas fluorescence to perform an image of the beam [1]. In the LEBT, no conventional beam position monitor (BPM) is installed, i.e. based on the RF technology. However, the information on the position can be provided by the measurement of the centroid on the beam distribution profile. But to provide this measurement in the ESS general coordinate system, additional knowledge to the usual NPM imaging system has to be provided. In the following, we will present the design and the performance of the NPM for the LEBT, matching the requirement of the beam size and beam position. The requirements for the profile, the beam size and the beam position are summarized in the table 1

NPM DESIGN FOR THE LEBT

The NPM for the LEBT is based on imaging the proton induced fluorescence. It is composed of an optical system and a camera. The design of the system has been optimised to

* cyrille.thomas@ess.se

Table 1: Requirements for the Beam Profile, Size and Position

Profile Error (%)	r.m.s Size (%)	Beam Position Error (mm)
1	10	0.1

satisfy several criteria, based on point spread function, depth of field, capture efficiency, and field of view, sensitivity and signal to noise ratio across the range of current from 1 mA to 70 mA. All these performance criteria together with the geometry of the vacuum chamber define the optical system the sensitivity and the size of the camera sensor. To start with, the viewport size is defined as a requirement to be large enough so that it offers a minimum numerical aperture of $NA = 0.22$. This condition is matched by design with a viewport on a CF DN-100 flange, with 105 mm aperture, and with the distance to the centre of the vacuum chamber, 230 mm. The main objective for the requirement on the numerical aperture of the viewport of the NPM is to provide a potential capture of 1% of the total solid angle of the emitted photons, 4π . In the design of the optical system, the object numerical aperture may match the one offered by the viewport. However, this might not always be possible to achieve due to additional constraint.

In the following we will expose how the optical system has been selected to match as close as possible the expected performance.

In addition to the optical performance for imaging, the system is expected to deliver information on the centre of the beam with respect to the centre of the vacuum chamber, i.e. in the ESS general coordinate system. This can be achieved on the condition that the position of the sensor with respect to the focal plan image is known with the required accuracy. We will present how this can be achieved with the required precision.

System Optimisation for the Imaging Performance

The system schematic is shown in the Fig. 1. The source is composed of point sources distributed with the proton beam transverse distribution and linearly along the beam path, and which are emitting uniformly over 4π solid angle. The photon flux emitted by the source per unit length of interaction along the beam path, the gas fluorescence excited by the protons, can be estimated by:

$$N_{ph} = \sigma_f \frac{P_g}{RT} N_a \quad (1)$$

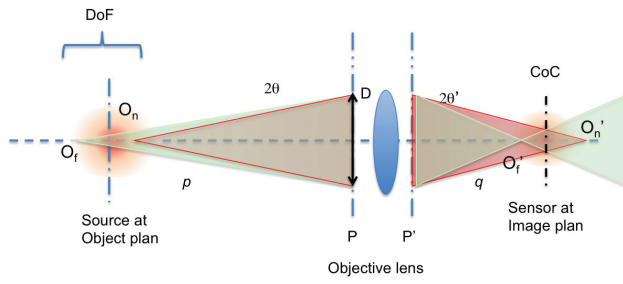


Figure 1: Imaging system schematic for the beam induced fluorescence. The point sources O_n and O_f are imaged in O_n' and O_f' respectively; their cones of light project on the camera sensor such that their extreme rays coincide with the CoC; the distance between O_f and O_n represents the DoF. The objective lens aperture, D , defines how much power it can transmit through; the distances p and q from object and source, to object and source principal plans respectively, define the magnification for the conjugate points.

where σ_f is the cross-section for the fluorescence, P_g is the pressure of the gas, \bar{R} is the gas constant, T the temperature of the gas, and N_a the Avogadro constant. The typical cross-section for the hydrogen gas excited by protons [2], at 75 keV over the transition $1s$ to $3p$, is $\sigma_{f:1s-3p} \approx 0.14 \times 10^{-16} \text{cm}^2$. This excitation transition induces fluorescence of the hydrogen at the Balmer α ray at $\lambda \approx 656.2 \text{nm}$. In the LEBT the gas pressure is expected to be $P_g = 10^{-5} \text{mbar}$ at room temperature $T=295 \text{K}$. So the total number of photons expected from the source is $N_{ph} \approx 2.45 \times 10^{10} \text{cm}^{-1}$.

The image of the proton beam is performed by the objective lens, from which the principle characteristics are: the physical aperture, D , which combined the focal length, f , gives the effective numerical aperture (NA, eq. ??), and in addition with the distance to the object gives the effective numerical aperture (NA_o Eq. 6); the Depth of Field, (DoF, Eq. 8), depends on the circle of confusion (CoC and on NA.

The expressions used for the selection of the objective lens are the following [3]:

$$m = \frac{q}{p} = \frac{s_{CCD}}{s_{\text{object}}} \quad (2)$$

$$f = \frac{pm}{m+1} \quad (3)$$

$$N = \frac{f}{D} \quad (4)$$

$$NA = n \sin(\theta) = n \sin\left(\arctan\left(\frac{D}{2f}\right)\right) \approx \frac{D}{2f} \quad (5)$$

$$NA_o = \frac{D}{2f} \frac{m}{m+1} \quad (6)$$

$$R = 1.22 \frac{\lambda}{NA_o} \quad (7)$$

$$\text{DoF} = \frac{2N\text{CoC}(m+1)}{m^2 - \left(\frac{N\text{CoC}}{f}\right)^2} \quad (8)$$

m is the lateral magnification of the objective lens¹, which can be calculated with either the distances object - principal plane object and image - principal plane image, p and q respectively, or with the size of the field of view and the size of the camera sensor; NA_o is the numerical aperture object; R is the diffraction limited of the Airy radius, image of a point source; λ is the photons source wavelength through the lens; $N = f/D$ is the f -number of the objective lens.

The source is composed of distributed point sources emitting over 4π solid angle, the fraction of the power of light reaching the sensor is given by:

$$T_l = \sin\left(\frac{\theta}{2}\right)^2 \approx \frac{NA_o^2}{4} \quad (9)$$

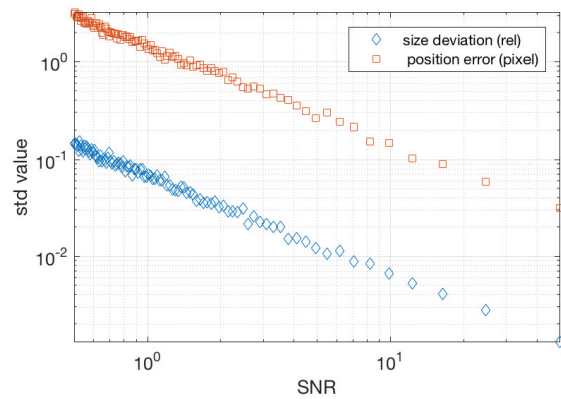


Figure 2: Deviation from the r.m.s value and centre of mass: the results come from a fit of a Gaussian with added noise.

In order to match the requirements shown in table 1, the optical system should deliver the following performance:

the profile measurement error depends on the signal to noise ratio (SNR) which can be evaluated as²

$$\text{SNR} = \frac{\eta \mu_p}{\sqrt{\eta \mu_p + \sigma_d^2 + \sigma_q^2/K}} \quad (10)$$

where η is the quantum efficiency, μ_p the photon flux per pixel, σ_d the r.m.s dark noise, σ_q the r.m.s digital noise, and K the overall sensor gain.

For an ideal sensor, where $\eta \mu_p \gg \sigma_d^2 + \sigma_q^2/K$, $\text{SNR} = \sqrt{\eta \mu_p}$.

Assuming the beam to be Gaussian, and analyses by a standard non-linear fit algorithm, one can evaluate the deviation of the measurement of the profile as function of SNR. Figure 2 presents the results of such an analysis. The figure shows the standard deviation of series of fit of a Gaussian with added noise. The result shows the deviation from the r.m.s size is less than 10% and the position measured with the centre of mass of the Gaussian is less than a pixel both for $\text{SNR} > 1$. This implies that the requirement on the

¹ the magnification is chosen here to be absolute: $m = |m|$

² Eq. 10 is based on EMVA Standard 1288, Standard for Characterization of Image Sensors and Cameras

profile error is likely to be matched with an optical system performance presenting a large T_l .

In addition, the accuracy of the width measurement is also influenced by R and CoC, which are diffraction and geometrical quantities accounting for the size of a point source on the sensor. This size is called the point spread function, σ_{PSF} . Assuming a Gaussian distribution of the point spread function, the measured size can be expressed as:

$$\sigma_m = \sqrt{\sigma_{b,m} + \sigma_{PSF}} \quad (11)$$

where $\sigma_{b,m}$ is the image beam size.

Using Eq. 11, one can express the minimum relative size for which the requirement on the beam size precision, Δ , is satisfied when

$$\left(\frac{\sigma_{PSF}}{\sigma_{b,m}}\right) < \sqrt{2\Delta} \quad (12)$$

The last the requirement on the position is discussed in the next sub-section. With Eq. 12 and 10, one can use the equations from 2 to 9 to select the optical system for the LEBT NPM.

Table 2 shows the results from applying the formulae for the selection of the lens, based on the vacuum chamber geometry, and several standard camera sensor sizes. We have started to select sensor sizes to define the magnification which satisfies a FOV equal to $7 \times \sigma_b$, taking the largest expected beam size, to ensure the wings of the beam distribution to be imaged. This guaranties the least uncertainty on the fit. Once m is defined, one can set the focal length, using the known distance of the lens to the beam. Then one can select the aperture of the lens and then define NA_o , R and T_l . Finally with selection of the acceptable circle of confusion, DoF is defined. So with all this, we need to select a lens which provides the largest T_l together with the largest DoF, and the smallest R . The calculation shown in Tab. 2 shows that a typical 4/3" sensor associated with a with $f = 50$ mm objective lens opening at $N = 1.4$ would be suitable for the NPM in the LEBT. It would allow to have $T_l \approx 10^{-3}$, and thus from Eq. 1, the total number of photon on the sensor is $N_{sensor} = N_{ph}(h_{CCD}/m)T_l \approx 135 \times 10^6$. In turn, if we assume almost 100% of the intensity is distributed over 6σ , the average number of photons per pixel is $\mu_p = N_{sensor} \Delta_{px}/(6m\sigma_{b,m})$, with Δ_{px} the pixel size. So from Eq. 10 one can deduce $SNR = \sqrt{N_{sensor} \Delta_{px}/(6m\sigma_{b,m})} \sqrt{\eta}$. A typical camera with a 4/3" sensor is 17×13 mm² and $\Delta_{px} = 5$ μ m. For a beam size $\sigma_b = 10$ mm, $m = 0.24$, $SNR = 216 \sqrt{\eta}$, implying that the profile requirement is satisfied for most camera quantum efficiency. In addition, with $\sigma_{PSF} < CoC = 0.1$ mm, the requirement on the size accuracy is also satisfied for any r.m.s beam size larger than 1 mm.

System Design for BPM Performance

The beam position requirement implies that the NPM has to return a position of the beam within and error less 0.1 mm

Table 2: Lens performance and characteristics for given values of the sensor size, with the object at $p = 250$ mm from the lens, $N = 1.4$, CoC = 0.1 mm, $\lambda = 0.5$ μ m, and with FoV = 70 mm

Sensor size (mm)	m	f (mm)	DOF (mm)	NA_o ($\times 10^{-2}$)	R (μ m)	T_l ($\times 10^{-4}$)
7	0.1	22.7	31.2	3.21	19	2.6
9	0.13	28.5	19.3	4.0	15	4.1
13	0.19	39.2	9.7	5.5	11	7.7
15	0.21	44.1	7.5	6.2	9.8	9.7
17	0.24	48.9	6.0	6.9	8.8	12
22	0.31	59.8	3.8	8.5	7.2	18
24	0.34	63.8	3.2	9	6.8	20
36	0.51	84.9	1.6	12	5.1	36

and with respect to the centre of the vacuum chamber in the ESS general coordinate system. In order to achieve this, one has to position the optical axis of each of the imaging systems of the NPM in the ESS general coordinate system, and then, the absolute position of the image sensor has to be known with respect to the focal plan. This is achieved firstly by the use of an commercial objective lens which has a focusing mechanism and infinity focus position marked, and then by adding an encoded motor to control the focus of the lens. With this mechanical assembly, the position of the sensor with respect to the focal plan is always known within a high accuracy provided by the encoder resolution. As a result the position of the object plan is also known with the same precision, by means of the lens equation.

$$XY = ff' \quad (13)$$

with $X = p - f$ and $Y = q - f$ are the distances from object and image to the focal plans object and image respectively, and f and f' are the focal lengths object and image respectively. Figure 3 shows the object position from the front flange of the lens, as function of the image sensor position. On the right axis, the accuracy required on the knowledge of the position of the sensor for $\Delta p = 0.1$ mm.

SYSTEM UNIT PROTOTYPE

The design of the NPM is made of two identical units, composed of a camera and motorised lens controlling the focus, assembled in a mechanical assembly, design to hold the unit in position, and permit its alignment in the coordinate system. The motor for the lens has an encoder reporting the position of the C-mount camera sensor with respect to the focal plane. The motor is integrated in the EPICS control system, and it is driven by a GeoBrick³ for the prototype. The motor controller will migrate to the ESS standard motor con-

³ <http://deltatau.co.uk/geo-brick-iv/>

troller based on EtherCAT Technology⁴. Both controllers are integrated into EPICS control. The lens selected is a 50 mm fixed focal length, F# 1.4, commercially available. The camera is GiGE-vision, allied vision camera GT 3300, selected for the sensor size to match magnification and field of view, and existing EPICS control. The motors are standard 2-phase stepper motors, and together with the encoder and the appropriated linear mechanics provide the required step motion to be less than 2 μ m.

ALIGNMENT AND CALIBRATION

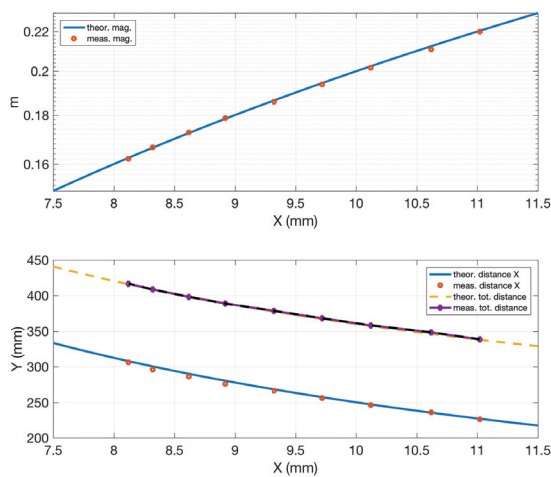


Figure 3: Optical system calibration of the magnification (top graph), and prediction of the distance of the object to the focal plane, and to the image position (bottom graph). The continuous and dash lines are extracted from lens equations, knowing the mechanical offset of 5 mm introduced to image the beam at the nominal 230 mm from the viewport flange.

The alignment of the NPM is done in several steps. Firstly, the optical axis is measured, with the support of the Alignment and Survey team. The measurement consists in putting a fiducialised target in the center of the camera image at two points distances at least from the camera. These points are measured in the ESS coordinate system with the Alignment instrument⁵. Then the fiducials on the NPM unit assembly are used to measure the position of the camera. These points are used to align the camera so that the optical axis intercepts orthogonally the beam axis. With this procedure the points along the optical axis are projected within one pixels or less on the center of the camera sensor. Then the angular error on the camera alignment is expected to be less than 700 μ rad for two points measured at 250 mm and 350 mm from the lens.

⁴ www.beckhoff.com/EtherCAT

⁵ LEICA ABSOLUTE TRACKER AT960-LR

The resulting beam position error measured at the centre of the image for a nominal beam distance at 250 mm from the lens is less than 20 μ m. Measurement performed after alignment of the unit shows a deviation from the reference axis of the order of 100 μ m across the 90 mm measured focusing range of the camera.

The calibration of the unit brings knowledge on the magnification, the distance of the object to the image, as function of the known distance camera sensor to focal plane. The image sensor is located at the standard C-mount distance from the flange of the lens, which is located with high accuracy (< 5 μ m) with the Alignment tool. The magnification is provided by measurement on a calibrated target, which is moved along the optical axis. The encoder position which has been calibrated so that it reports the distance image to focal plane, is recorded for each of the calibration target. The results of the calculation of the magnification and the corresponding total distance is shown in Fig. 3. The agreement with the theoretical prediction is better than 1%.

The resolution of the unit is measured by means of a sharp edged target. Detail of the measurement and calculation is not shown, however, the measured point spread function presents an r.m.s width of the order of 10 μ m. The sensitivity of the unit remains to be measured.

CONCLUDING REMARKS

We have designed and built a prototype of the first of the NPM for the ESS linac. This profile monitor to be installed in the LEBT section of the ESS linac, has received the additional requirement to be a beam position monitor. The prototype has been tested successfully. The camera resolution, the field of view all match the requirements. The requirement on the beam position is also matched. The alignment procedure has proven that the centre of the image can be within 100 μ m from the accelerator beam axis defined in the ESS general coordinate system.

ACKNOWLEDGMENTS

We would like to thank the Alignment and Survey team at ESS which has been supporting us in the design and for the qualification of the alignment procedure.

REFERENCES

- [1] P Forck and A Bank. Residual Gas Fluorescence for Profile Measurements at the GSI UNILAC. In *EPAC*, 2002.
- [2] E. Fitchard, A.L. Ford, and J.F. Reading. Hydrogene-atom excitation and ionization by proton impact in the 50- to 200-keV energy region. *Physical Review A*, 16, 1977.
- [3] L. Larmore. *Introduction to photographic principles*. Dover Publications, 1965.